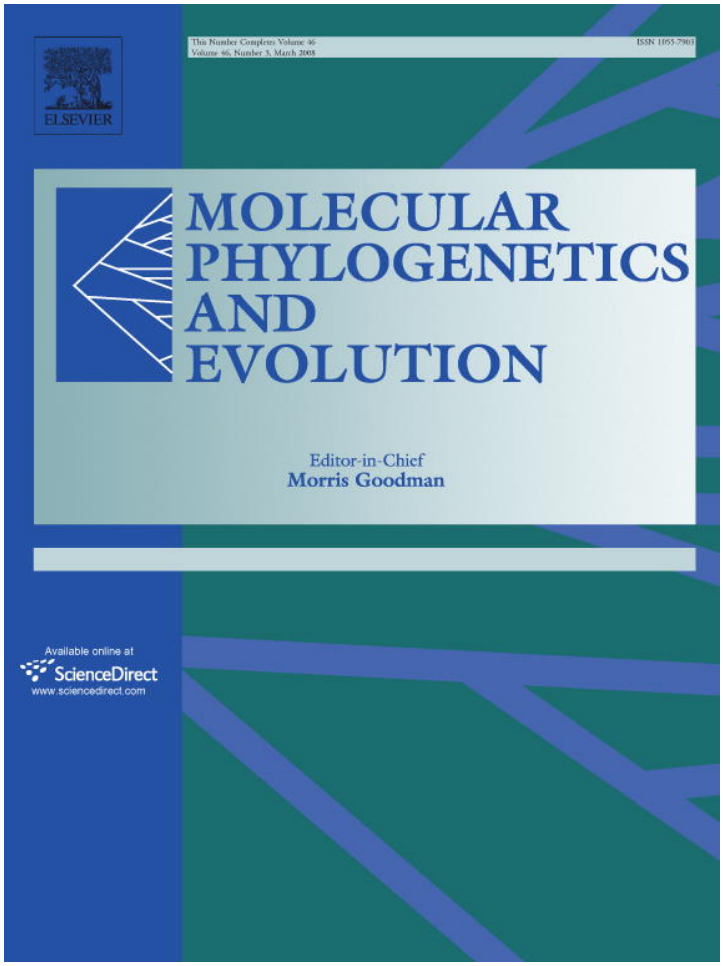

Available online at www.sciencedirect.com
ScienceDirect
Molecular Phylogenetics and Evolution 46 (2008) 844–862
MOLECULAR PHYLOGENETICS AND EVOLUTION
www.elsevier.com/locate/ympev

Inferences on the phylogeography of the fungal pathogen *Heterobasidion annosum*, including evidence of interspecific horizontal genetic transfer and of human-mediated, long-range dispersal

R.E. Linzer [a], W.J. Otrosina [b], P. Gonthier [c], J. Bruhn [d], G. Laflamme [e], G. Bussières [f], M. Garbelotto [a,*]

[a] *Department of Environmental Science, Policy and Management—Ecosystem Sciences Division, University of California at Berkeley, 137 Mulford Hall # 3114, Berkeley, CA 94720, USA*
[b] *USDA Forest Service, 320 Green Street, Athens, GA 30602, USA*
[c] *Department of Exploitation and Protection of the Agricultural and Forestry Resources—Plant Pathology, University of Torino, Via L. da Vinci 44, I-10095 Grugliasco, Italy*
[d] *University of Missouri—Columbia, Division of Plant Sciences, 108 Waters Hall, Columbia, MO 65211, USA*
[e] *Canadian Forest Service, 1055 P.E.P.S. Str., Québec, Que., Canada G1V 4C7*
[f] *Université Laval, Centre de recherche en biologie forestière, Faculté de foresterie et de géomatique, Ste-Foy, Que., Canada G1K 7P4*

Received 29 November 2006; revised 10 October 2007; accepted 11 December 2007
Available online 1 February 2008

Abstract

Fungi in the basidiomycete species complex *Heterobasidion annosum* are significant root-rot pathogens of conifers throughout the northern hemisphere. We utilize a multilocus phylogenetic approach to examine hypotheses regarding the evolution and divergence of two *Heterobasidion* taxa associated with pines: the Eurasian *H. annosum sensu stricto* and the North American *H. annosum* P intersterility group (ISG). Using DNA sequence information from portions of two nuclear and two mitochondrial loci, we infer phylogenetic relationships via parsimony, Bayesian and median-joining network analysis. Analysis of isolates representative of the entire known geographic range of the two taxa results in monophyletic sister Eurasian and North American lineages, with North America further subdivided into eastern and western clades. Genetically anomalous isolates from the Italian presidential estate of Castelporziano are always part of a North American clade and group with eastern North America, upholding the hypothesis of recent, anthropogenically mediated dispersal. P ISG isolates from Mexico have phylogenetic affinity with both eastern and western North America. Results for an insertion in the mitochondrial rDNA suggest this molecule was obtained from the *Heterobasidion* S ISG, a taxon sympatric with the P ISG in western North America. These data are compatible with an eastern Eurasian origin of the species, followed by dispersal of two sister taxa into western Eurasia and into eastern North America over a Beringean land bridge, a pattern echoed in the phylogeography of other conifer-associated basidiomycetes.

Keywords: Basidiomycota; Biogeography; Eurasia; North America; Intersterility group; Median-joining network; *Pinus*; Phylogeny; Phylogeography

1. Introduction

Positioned at the intersection of traditional cladistics and microevolutionary approaches, intraspecific phylogeography can be used to understand forces shaping genetic lineages from ancient to recent time (Avise, 2000). The current proliferation of studies that apply phylogeographic methods to explain the histories of closely related fungal lineages has yielded evolutionary data at both recent and ancient temporal scales. Phylogeographic approaches have uncovered distinct continental groupings within fungal species due to ancient vicariance or dispersal events (Johannesson and Stenlid, 2003; Oda et al., 2004; Petersen and

* Corresponding author. Fax: +1 510 643 5098.
E-mail address: matteo@nature.berkeley.edu (M. Garbelotto).

1055-7903/$ - see front matter © 2008 Published by Elsevier Inc.
doi:10.1016/j.ympev.2007.12.010

Hughes, 2003). Intraspecific fungal phylogeography can also be used to uncover recent events that shape fungal lineages, such as long-distance, human-mediated dispersal of fungi (Coetzee et al., 2001; Fisher et al., 2001; Kauserud et al., 2004; Methven et al., 2000; Vilgalys and Sun, 1994; Zervakis et al., 2004). Moreover, straightforward biological and morphological species recognition is often insufficient for fungal classification. Fungal phylogeographic studies may assist in a systematic reevaluation of evolutionary relationships within and among previously designated taxonomic groups (Crouch et al., 2006; Kasuga et al., 2003; Wu et al., 2000).

The forest pathogen *Heterobasidion annosum* (Fr.) Bref. *sensu lato* (*s.l.*) has become an important model system for the analysis of fungal-lineage diversification (Kohn, 2005). *H. annosum s.l.* is among the most significant pathogens in northern temperate coniferous forests worldwide. This basidiomycete is widely distributed and causes root- and heart-rot of more than 200 woody plant taxa, primarily coniferous trees (Korhonen and Stenlid, 1998). The fungus is indigenous in many areas and is an important ecological factor involved in nutrient cycling, forest regeneration and forest succession (Garbelotto, 2004). *Heterobasidion* root disease, however, can be exacerbated by some forest management practices including precommercial thinning, logging and plantation forestry (Pratt and Greig, 1988; Stenlid and Swedjemark, 1988).

Although *H. annosum s.l.* was originally classified as a single species, fungi formerly grouped under this name are now characterized as a complex of genetically and phenotypically distinct taxa. Mating studies revealed three *H. annosum* intersterility groups (ISGs): S, F and P (Capretti et al., 1990; Korhonen, 1978). These taxa are characterized by partial morphological differentiation and host preference, with some overlap among ISGs. Intersterility among groups is incomplete, with success of inter-ISG crosses ranging between 0% and 72% (Korhonen et al., 1992; Stenlid and Karlsson, 1991). While mating barriers are weak between allopatric populations belonging to different ISGs, they are strong between sympatric ISGs, suggesting intersterility can be subject to selection to reinforce genetic isolation between diverging lineages (Korhonen et al., 1992; Stenlid and Karlsson, 1991).

Using molecular methods, at least five taxa have been delimited within the *H. annosum* species complex: Eurasian F, S and P ISGs and North American S and P ISGs (Garbelotto et al., 1996; Harrington et al., 1998; Johannesson and Stenlid, 2003; Karlsson and Stenlid, 1991; Korhonen and Dai, 2005; Otrosina et al., 1993). The Eurasian P ISG is currently referred to as *Heterobasidion annosum sensu stricto (s.s.)*. The F and S ISG lineages from Europe have been designated as separate taxonomic species—*H. abietinum* Niemelä and Korhonen and *H. parviporum* Niemelä and Korhonen, respectively (Niemelä and Korhonen, 1998). Several evolutionary hypotheses have been formulated regarding the global history of *Heterobasidion*. A Eurasian origin for the complex has been suggested, followed by either ancient spread into North American during the late Tertiary or more recent colonization (Korhonen and Dai, 2005; Otrosina et al., 1993).

Although there have been numerous studies examining population substructure and relationships among taxa within the *H. annosum (s.l.)* species complex, an in-depth study of the most widespread group, the P ISG which generally attacks pines in Eurasia and North America, is still lacking. Although accumulating evidence suggests that the North American P ISG and *H. annosum s.s.* represent distinct taxa, they nevertheless share more similarities than exist between other ISGs. They are both predominantly found on pines, although they also infect a broad range of hosts, and *in vitro* crosses between isolates of the two taxa are almost entirely interfertile (Chase and Ullrich, 1990; Stenlid and Karlsson, 1991). They share a similar mode of pathogenicity, as P ISG genotypes in both continents kill the cambium and colonize the outer sapwood of roots (Stenlid and Redfern, 1998). The European *H. annosum s.s.* has been distinguished from the North American P ISG by analysis of three different molecular markers: neutral allozymes, pectic enzymes and ITS/IGS DNA sequences (Karlsson and Stenlid, 1991; Otrosina et al., 1993; Harrington et al., 1998). Sequences of a family of four paralogous manganese peroxidase genes, a wood-degradation enzyme, show no overlapping sequences between the two taxa, with two paralogs belonging exclusively to one or the other (Maijala et al., 2003). By contrast, molecular phylogenetic analyses of the wood-degradation enzyme, laccase, do not clearly differentiate the two taxa (Asiegbu et al., 2004). Not only is the relationship between the two taxa and their ancient evolutionary history unclear, but the taxonomic status of the *Heterobasidion* P ISG lineages (European *H. annosum s.s.* and North American *Heterobasidion* P ISG) remains an open question (Korhonen and Dai, 2005). The P ISG evolutionary history and distribution may also have been affected by relatively recent events. A natural, stable SP hybrid has been isolated in North America (Garbelotto et al., 1996, 2004), and a phylogenetic study including several isolates from a pine forest near Rome strongly suggested a North American origin for those collections (Gonthier et al., 2004). Finally, there is currently no information regarding phylogenetic relationships among P ISG populations from different intracontinental regions.

In this study, we use a phylogeographic approach to address evolutionary and ecological questions regarding the *H. annosum s.s.* and the North American *Heterobasidion* P ISG at both recent and ancient time scales. Our objectives were: (1) to undertake a multilocus analysis of the P ISG (*H. annosum s.s.* and North American *Heterobasidion* P ISG) utilizing extensive worldwide samples to delimit phylogeographic structure from the intra- to the intercontinental scale, (2) to examine previous hypotheses about the origin and biogeography of the P ISG in ancient evolu-

tionary time, (3) to evaluate the possibility of inter-ISG genetic exchanges among taxa within the *Heterobasidion* complex, and (4) to examine the hypothesis of a recent introduction from the US into Italy.

2. Materials and methods

2.1. Study sites and isolates

We analyzed 133 *Heterobasidion* isolates from 44 different sites in North America and Eurasia. Among these are seven putative North American isolates from Castelporziano, near Rome, four *H. parviporum*, four *H. abietinum*, eight western US S ISG isolates (heretofore referred to as "S ISG"), and one *H. insulare* (Murr.) Ryv. isolate as the outgroup. *H. insulare* was chosen as outgroup based on previous results from ITS/IGS and laccase genes (Harrington et al., 1998; Asiegbu et al., 2004). Detailed isolate information is presented in Table 1; nomenclature is per Niemelä and Korhonen (1998). This study includes isolates from the entire known distribution of the pathogen in pine. For the North American P ISG, this ranges from southern Canada to central Mexico and from the Atlantic to the Pacific coast. For the Eurasian *H. annosum s.s.*, this ranges from Italy to Scandinavia and from the United Kingdom to the Altai region in southwestern Siberia. Notably, we also included isolates from the US states of Missouri and Wisconsin, a little-studied region of this pathogen's distribution.

2.2. DNA extraction

DNA was extracted by picking a few hyphal tips from the edge of colonies growing on malt extract agar, suspending them in 0.1× Tris–EDTA buffer, and subjecting the suspension to three consecutive freeze–thaw cycles, alternating 2 min in a metal block on dry ice and 2 min at 75 °C, with a final incubation at 75 °C for 15 min. DNA from herbarium specimens was obtained by excising 100–150 mg of the dry basidiocarp with a sterile blade, excluding any tissue from the outside surface of the sample to minimize contamination. Basidiocarp fragments were placed in individual 2 mL screw-top vials with two 6.35 mm sterile glass beads and pulverized in a Mixer Mill MM 301 (Retsch, Inc., Newtown, PA) set at 30 beats per second. Basidiocarp tissue was completely powdered after 0.5–2 min. Total DNA was then extracted from the pulverized tissue using a modified cetyltrimethyl ammonium bromide (CTAB) protocol, as described in Hayden et al. (2004).

2.3. PCR, sequencing and alignment

We sequenced PCR amplicons of two nuclear regions: coding and non-coding portions of glyceraldehyde 3-phosphate dehydrogenase (GPD) and elongation factor 1-α (EFA), and two mitochondrial loci: part of the ATP synthase subunit 6 coding region (ATP) and a non-coding insertion in the ML5–ML6 region of the mitochondrial large rRNA gene. The rDNA insertion is present in two non-homologous forms of approximately 1.6 or 1.8 kb in length. Notably, all tested Eurasian *H. annosum s.s.* isolates lack this insertion. Though these factors complicate the analysis of this locus, both forms have the highest observed genetic variability of any study locus and yield additional information about relationships between isolates in which the insertion is found. PCR primers for all loci are listed in Table 2.

PCR was performed in the following 25 μl reaction mixture: 1× buffer, 0.2 mM dNTPs, 1.25 U *Taq* (Promega Corp. Madison, WI), 2.0 mM $MgCl_2$ (Invitrogen Corp. Carlsbad, CA), 0.50 μM each non-degenerate primer or 0.64 μM each degenerate primer (Table 2), and between 50 and 100 ng DNA or 7 μl hyphal tip-extracted DNA (above). The PCR programs used were: 95 °C 3:00; 35 cycles of: 95 °C 0:40 (50 °C for ATP, 52 °C for GPD, 66 °C for EFA) 0:55, 72 °C 0:55; 72 °C 7:00. As the rDNA insertion amplicons are 1.6 kb or greater in length, an extended PCR was used as described in Gonthier et al. (2001). When no PCR products were visible on an agarose gel for herbarium specimens, we used the reaction programs above with a modified 25 μl PCR mix: 1× buffer, 1.25 U Platinum *Taq*, 2.0 mM $MgCl_2$(all Invitrogen Corp. Carlsbad, CA), 0.2 mM dNTPs, 0.50 μM each non-degenerate primer or 0.64 μM each degenerate primer and 5–8 μl 1:10-diluted DNA. An identical second round of PCR was then performed using 2.5 μl undiluted PCR product as the template. PCR products were cleaned with the QIAquick PCR clean-up kit (Qiagen Inc. Valencia, CA). Both forward and reverse strands were sequenced using the above PCR primers and BigDye Terminator (version 3.1) chemistry, according to manufacturer's protocols, but using 25% of the recommended reaction (ABI Foster City, CA). Reactions were precipitated and products visualized on an ABI 3100 Prism capillary sequencer, following ABI protocols. Sequences were edited and aligned in Sequencher (Gene Codes Corp., Ann Arbor, MI), and alignments were manually refined using Se–Al where necessary (Rambaut, 1996). The rDNA insertion could not be sequenced through; 5′ and 3′ reads were concatenated for further analysis.

Six heterokaryotic isolates that exhibited double peaks in forward and reverse sequences were cloned before sequencing using the TOPO TA cloning kit and manufacturer-provided protocols (Invitrogen Corp., Carlsbad, CA). Not all putative heterozygotes could be cloned, so we cloned those from areas with little geographic representation. Eight clones for each reaction were picked with a sterile toothpick and touched to a PCR mix (above) with sterile water in place of DNA template and using T7 and M13 Reverse primers. To release plasmid DNA, each reaction was incubated for 10 min at 95 °C before amplification according to kit protocol. Products were sequenced as above. Cloned alleles were chosen randomly for inclusion in phylogenetic analysis.

Table 1
Isolates

Isolate	Geographic origin	*Heterobasidion* Taxon	Collector[a]	NCBI GenBank Accession No. ATP[b,c,d]	EFA[c]	GPD[c]	MRI seg1[c]	MRI seg2[c]	MRI size (kb)[c]
98007	Lac La Blanche, Québec, Canada	*H. annosum* P	GB&GL	EU189963	EU189973	EU190083	EU190187	EU190188	1.8
98008	Lac La Blanche, Québec, Canada	*H. annosum* P	GB&GL	EU189963	EU189974	EU190084	EU190189	EU190190	1.8
98011	Lac La Blanche, Québec, Canada	*H. annosum* P	GB&GL	EU189963	EU189975	EU190085	EU190191	EU190192	1.8
98027	Lac La Blanche, Québec, Canada	*H. annosum* P	GB&GL	EU189963	EU189976	EU190086	EU190193	EU190194	1.8
98028	Lac La Blanche, Québec, Canada	*H. annosum* P	GB&GL	EU189963	EU189977	EU190087	EU190195	EU190196	1.8
98029	Lac La Blanche, Québec, Canada	*H. annosum* P	GB&GL	EU189963	EU189978	EU190088	EU190197	EU190198	1.8
98034	Harrington, Québec, Canada	*H. annosum* P	GB&GL	EU189963	EU189979	EU190089	EU190199	EU190200	1.8
98001	Cushing, Québec, Canada	*H. annosum* P	GB&GL	EU189964	EU189980	EU190090	—	—	—
98002	Cushing, Québec, Canada	*H. annosum* P	GB&GL	EU189964	EU189981	EU190091	EU190291	EU190292	1.6
98003	Cushing, Québec, Canada	*H. annosum* P	GB&GL	EU189963	EU189982	EU190092	EU190201	EU190202	1.8
98004	Cushing, Québec, Canada	*H. annosum* P	GB&GL	EU189963	—	EU190093	EU190203	EU190204	1.8
98005	Cushing, Québec, Canada	*H. annosum* P	GB&GL	EU189963	EU189983	EU190094	EU190205	EU190206	1.8
98006	Cushing, Québec, Canada	*H. annosum* P	GB&GL	DQ916074	DQ916086	DQ916103	EU190293	EU190294	1.6
98035	Cushing, Québec, Canada	*H. annosum* P	GB&GL	EU189963	EU189984	EU190095	EU190207	EU190208	1.8
98036	Cushing, Québec, Canada	*H. annosum* P	GB&GL	EU189963	EU189985	EU190096	EU190209	EU190210	1.8
98038	Cushing, Québec, Canada	*H. annosum* P	GB&GL	EU189963	EU189986	EU190097	EU190211	EU190212	1.8
98040	Cushing, Québec, Canada	*H. annosum* P	GB&GL	EU189963	EU189987	EU190098	EU190213	EU190214	1.8
98041	Cushing, Québec, Canada	*H. annosum* P	GB&GL	EU189964	EU189988	EU190099	EU190295	EU190296	1.6
98042	Cushing, Québec, Canada	*H. annosum* P	GB&GL	EU189964	EU189989	EU190100	EU190297	EU190298	1.6
98012	Forêt Larose, Ontario, Canada	*H. annosum* P	GB&GL	DQ916072	DQ916086	DQ916104	—	—	—
98014	Forêt Larose, Ontario, Canada	*H. annosum* P	GB&GL	—	EU189990	EU190101	EU190217	EU190218	1.8
98015	Forêt Larose, Ontario, Canada	*H. annosum* P	GB&GL	EU189963	EU189991	EU190102	EU190219	EU190220	1.8
98016	Forêt Larose, Ontario, Canada	*H. annosum* P	GB&GL	EU189963	EU189992	EU190103	EU190221	EU190222	1.8
98017	Forêt Larose, Ontario, Canada	*H. annosum* P	GB&GL	EU189963	EU189993	EU190104	EU190223	EU190224	1.8
98018	Forêt Larose, Ontario, Canada	*H. annosum* P	GB&GL	EU189963	EU189994	EU190105	EU190225	EU190226	1.8
2-1-3	Savannah River, SC, US	*H. annosum* P	WO	EU189963	EU189995	EU190106	EU190227	EU190228	1.8
4-2-1	Savannah River, SC, US	*H. annosum* P	WO	EU189965	EU189996	EU190107	EU190229	EU190230	1.8
351-1	Savannah River, SC, US	*H. annosum* P	WO	EU189963	EU189997	EU190108	EU190231	EU190232	1.8
323	Savannah River, SC, US	*H. annosum* P	WO	EU189963	EU189998	EU190109	—	—	—
365	Savannah River, SC, US	*H. annosum* P	WO	DQ916072	DQ916088	DQ916103	EU190233	EU190234	1.8
366	Savannah River, SC, US	*H. annosum* P	WO	EU189963	EU189999	—	EU190235	EU190236	1.8
427	Savannah River, SC, US	*H. annosum* P	WO	EU189963	EU190000	EU190110	EU190237	EU190238	1.8
1A	LA, US	*H. annosum* P	NH	DQ916073	DQ916086	DQ916102	EU190239	EU190240	1.8
1116-1	Georgia/Alabama, US	*H. annosum* P	WO	EU189963	EU190001	EU190111	EU190299	EU190300	1.6
11063B	Georgia/Alabama, US	*H. annosum* P	WO	EU189963	EU190002	EU190112	EU190241	EU190242	1.8
11115A	Georgia/Alabama, US	*H. annosum* P	WO	EU189963	EU190003	EU190113	EU190301	EU190302	1.6
12023B-2	Georgia/Alabama, US	*H. annosum* P	WO	EU189963	EU190004	EU190114	EU190303	EU190304	1.6
24086C	Georgia/Alabama, US	*H. annosum* P	WO	EU189963	EU190005	EU190115	EU190305	EU190306	1.6
Stop 1	Georgia/Alabama, US	*H. annosum* P	WO	EU189963	EU190006	EU190116	EU190243	EU190244	1.8
93-19	Adams Co., WI, US	*H. annosum* P	GS	EU189963	EU190007	EU190117	EU190245	EU190246	1.8
93-20	Adams Co., WI, US	*H. annosum* P	GS	EU189966	EU190008	EU190118	EU190247	EU190248	1.8
93-21	Adams Co., WI, US	*H. annosum* P	GS	EU189963	EU190009	EU190119	EU190249	EU190250	1.8
94-189	Iowa Co., WI, US	*H. annosum* P	GS	EU189966	EU190010	EU190120	EU190251	EU190252	1.8
94-190	Iowa Co., WI, US	*H. annosum* P	GS	EU189966	EU190011	EU190121	EU190253	EU190254	1.8
CL-3	Clear Lake, MO, US	*H. annosum* P	JB&MG	DQ916072	DQ916092	DQ916099	EU190255	EU190256	1.8
CL-4	Clear Lake, MO, US	*H. annosum* P	JB&MG	—	EU190012	EU190122	EU190307	EU190308	1.6

(*continued on next page*)

Table 1 (*continued*)

Isolate	Geographic origin	*Heterobasidion* Taxon	Collector[a]	NCBI GenBank Accession No.					
				ATP[b,c,d]	EFA[c]	GPD[c]	MRI seg1[c]	MRI seg2[c]	MRI size (kb)[e]
CL-5	Clear Lake, MO, US	*H. annosum* P	JB&MG	DQ916072	DQ916086	DQ916100	EU190309	EU190310	1.6
CL-6	Clear Lake, MO, US	*H. annosum* P	JB&MG	EU189963	EU190013	EU190123	EU190311	EU190312	1.6
Conk1	De Soto National Forest, MS, US	*H. annosum* P	WO	DQ916072	DQ916087	DQ916101	EU190257	EU190258	1.8
Conk2	De Soto National Forest, MS, US	*H. annosum* P	WO	EU189963	—	EU190124	EU190259	EU190260	1.8
Conk3	De Soto National Forest, MS, US	*H. annosum* P	WO	EU189963	EU190014	EU190125	EU190261	EU190262	1.8
305-4	Lassen National Forest, CA, US	*H. annosum* P	WO	DQ916075	DQ916090	DQ916102	EU190263	EU190264	1.8
310-7	Lassen National Forest, CA, US	*H. annosum* P	WO	EU189967	EU190015	EU190126	EU190265	EU190266	1.8
327-5	Fremont National Forest, CA, US	*H. annosum* P	WO	EU189967	EU190016	EU190127	—	—	—
340-3	Modoc National Forest, OR, US	*H. annosum* P	WO	DQ916075	DQ916089	DQ916102	EU190267	EU190268	1.8
344-6	Modoc National Forest, CA, US	*H. annosum* P	WO	EU189967	EU190017	EU190128	—	—	—
354-1	Modoc National Forest, CA, US	*H. annosum* P	WO	EU189967	EU190018	EU190129	EU190269	EU190270	1.8
382-5	San Bernardino N.F., CA, US	*H. annosum* P	WO	EU189967	EU190019	EU190130	EU190313	EU190314	1.6
390	San Bernardino N.F., CA, US	*H. annosum* P	WO	EU189967	EU190020	EU190131	—	—	—
390-5	San Bernardino N.F., CA, US	*H. annosum* P	WO	EU189967	EU190021	EU190132	—	—	—
398-2	San Bernardino N.F., CA, US	*H. annosum* P	WO	EU189963	EU190022	EU190133	—	—	—
T338	Modoc National Forest, CA, US	*H. annosum* P	WO	EU189967	EU190023	EU190134	EU190271	EU190272	1.8
9b2x1	CA, US	*H. annosum* P	MG	EU189967	EU190024	—	EU190315	EU190316	1.6
15a1x1	CA, US	*H. annosum* P	MG	EU189967	—	EU190135	—	—	—
15a3y2	CA, US	*H. annosum* P	MG	—	—	EU190136	EU190273	EU190274	1.8
c1	San Diego, CA, US	*H. annosum* P	MG	EU189967	EU190025	EU190137	EU190317	EU190318	1.6
a2	San Diego, CA, US	*H. annosum* P	MG	EU189967	EU190026	EU190138	EU190275	EU190276	1.8
c3	San Diego, CA, US	*H. annosum* P	MG	EU189967	EU190027	EU190139	EU190319	EU190320	1.6
c4	San Diego, CA, US	*H. annosum* P	MG	EU189967	EU190028	EU190140	EU190321	EU190322	1.6
a5	San Diego, CA, US	*H. annosum* P	MG	EU189967	EU190029	EU190141	—	—	—
c6	San Diego, CA, US	*H. annosum* P	MG	DQ916075	DQ916089	DQ916103	EU190323	EU190324	1.6
c7	San Diego, CA, US	*H. annosum* P	MG	EU189967	EU190030	EU190142	EU190325	EU190326	1.6
BBb	WA, US	*H. annosum* P	MG	EU189967	EU190031	EU190143	EU190277	EU190278	1.8
BBf	WA, US	*H. annosum* P	MG	EU189967	EU190032	—	—	—	—
BBh	WA, US	*H. annosum* P	MG	DQ916075	DQ916089	DQ916103	—	—	—
BBi	WA, US	*H. annosum* P	MG	EU189967	EU190033	—	—	—	—
LOP 43	Hidalgo, Mexico	*H. annosum* P	NHM	—	EU190034	—	—	—	—
NAV 464	Hidalgo, Mexico	*H. annosum* P	NHM	EU189963	EU190035	—	EU196137	EU196138	1.6
REU 120	Michoacan, Mexico	*H. annosum* P	NHM	EU189963	EU190036	EU190144	EU190279	EU190280	1.8
ROL 503	Mexico, Mexico	*H. annosum* P	NHM	EU189963	EU190037	—	EU190281	EU190282	1.8
CP0	Castelporziano, Italy	*H. annosum* P	PG	EU189963	EU190038	EU190145	EU190327	EU190328	1.6
CP2	Castelporziano, Italy	*H. annosum* P	NA	EU189963	EU190039	EU190146	EU190329	EU190330	1.6
CP3	Castelporziano, Italy	*H. annosum* P	NA	DQ916072	DQ916083	DQ916098	EU190331	EU190332	1.6
CP7	Castelporziano, Italy	*H. annosum* P	NA	EU189963	EU190040	EU190147	EU190333	EU190334	1.6
CP9	Castelporziano, Italy	*H. annosum* P	NA	DQ916072	DQ916084	DQ916098	EU190335	EU190336	1.6
CP15	Castelporziano, Italy	*H. annosum* P	NA	DQ916072	DQ916085	DQ916098	EU190337	EU190338	1.6
CP18	Castelporziano, Italy	*H. annosum* P	NA	EU189963	EU190041	EU190148	EU190339	EU190340	1.6
417P	Aymavilles, AO, Italy	*H. annosum* P	MG	EU189968	EU190042	EU190149	N/A	N/A	N/A
A216r	Aymavilles, AO, Italy	*H. annosum* P	PG	EU189968	—	EU190150	N/A	N/A	N/A
Cal1	Taverna, CZ, Italy	*H. annosum* P	NL	EU189968	EU190043	EU190151	N/A	N/A	N/A
Cal2	Rogliano, CS, Italy	*H. annosum* P	NL	EU189968	EU190044	EU190152	N/A	N/A	N/A
L1b	Gressan, AO, Italy	*H. annosum* P	PG	EU189969	EU190045	EU190153	N/A	N/A	N/A

P12p	Charvensod, AO, Italy	*H. annosum* P	PG	EU189968	EU190046	EU190154	N/A	N/A	N/A
T5	Tuscany, Italy	*H. annosum* P	PC	EU189968	EU190047	EU190155	N/A	N/A	N/A
95092	Podanin, Poland	*H. annosum* P	PL	EU189968	EU190048	EU190156	N/A	N/A	N/A
98297	Karkonoski National Park, Poland	*H. annosum* P	PL	EU189968	EU190049	EU190157	N/A	N/A	N/A
98307	Golabki, Poland	*H. annosum* P	PL	EU189968	EU190050	EU190158	N/A	N/A	N/A
203005	Rembertòw, Poland	*H. annosum* P	PL	EU189968	EU190051	EU190159	N/A	N/A	N/A
203006	Lipusz, Poland	*H. annosum* P	PL	EU189968	EU190052	EU190160	N/A	N/A	N/A
791200-1-2	Finland	*H. annosum* P	KK	DQ916071	DQ916077	DQ916093	N/A	N/A	N/A
810928-1-1	Finland	*H. annosum* P	KK	DQ916071	DQ916078	DQ916094	N/A	N/A	N/A
00-070/1	Altai, Siberia, Russia	*H. annosum* P	KK	EU189968	EU190053	EU190161	N/A	N/A	N/A
00-071/1	Altai, Siberia, Russia	*H. annosum* P	KK	EU189968	EU190054	EU190162	N/A	N/A	N/A
00-072/9	Altai, Siberia, Russia	*H. annosum* P	KK	EU189968	EU190055	—	N/A	N/A	N/A
00-073/2	Altai, Siberia, Russia	*H. annosum* P	KK	EU189968	EU190056	EU190163	N/A	N/A	N/A
02-022/3	Altai, Siberia, Russia	*H. annosum* P	KK	EU189968	EU190057	EU190164	N/A	N/A	N/A
02-023/1	Altai, Siberia, Russia	*H. annosum* P	KK	EU189968	EU190058	EU190165	N/A	N/A	N/A
02-030/5	Altai, Siberia, Russia	*H. annosum* P	KK	EU189968	EU190059	EU190166	N/A	N/A	N/A
02-031/1	Altai, Siberia, Russia	*H. annosum* P	KK	EU189968	EU190060	EU190167	N/A	N/A	N/A
E3.1	Co. Fermanagh, N. Ireland, UK	*H. annosum* P	WB	EU189968	EU190061	EU190168	N/A	N/A	N/A
E14.2	Co. Fermanagh, N. Ireland, UK	*H. annosum* P	WB	EU189968	EU190062	EU190169	N/A	N/A	N/A
E18.11.3	Co. Fermanagh, N. Ireland, UK	*H. annosum* P	WB	EU189968	EU190063	EU190170	N/A	N/A	N/A
L58.1	Lael Forest, Scotland, UK	*H. annosum* P	WB	EU189968	EU190064	EU190171	N/A	N/A	N/A
B13.4	Bennachie Forest, Scotland, UK	*H. annosum* P	WB	EU189968	EU190065	EU190172	N/A	N/A	N/A
B20.1	Bennachie Forest, Scotland, UK	*H. annosum* P	WB	EU189968	EU190066	EU190173	N/A	N/A	N/A
B3.22	Bennachie Forest, Scotland, UK	*H. annosum* P	WB	EU189968	—	EU190174	N/A	N/A	N/A
9a5z	CA, US	*H. annosum* S	MG	EU189970	EU190067	EU190175	EU190341	EU190342	1.6
9b4y	CA, US	*H. annosum* S	MG	EU189970	EU190068	EU190176	EU190343	EU190344	1.6
9c3y	CA, US	*H. annosum* S	MG	EU189970	EU190069	EU190177	EU190345	EU190346	1.6
11a2y1	CA, US	*H. annosum* S	MG	EU189970	EU190070	EU190178	—	—	—
11b4x	CA, US	*H. annosum* S	MG	EU189970	EU190071	EU190179	EU190347	EU190348	1.6
15c5x	CA, US	*H. annosum* S	MG	EU189970	—	—	EU190349	EU190350	1.6
230-3	Plumas National Forest, CA, US	*H. annosum* S	WO	EU189970	EU190073	EU190180	EU190283	EU190284	1.8
BBe	WA, US	*H. annosum* S	MG	EU189970	EU190074	EU190181	EU190351	EU190352	1.6
343F	Italy	*H. abietinum*	MG	EU189972	EU190075	—	—	—	—
365F	Italy	*H. abietinum*	MG	EU189972	EU190076	EU190182	EU190353	EU190354	1.6
1010	Italy	*H. abietinum*	MG	EU189972	EU190077	EU190183	EU190285	EU190286	1.8
1041	Italy	*H. abietinum*	MG	EU189971	EU190078	EU190184	EU190287	EU190288	1.8
307S	Italy	*H. parviporum*	MG	EU189972	EU190079	—	—	—	—
318S	Italy	*H. parviporum*	MG	EU189972	EU190080	—	EU190355	EU190355	1.6
181-18	Finland	*H. parviporum*		EU189972	EU190081	EU190185	—	—	—
433-1	Germany	*H. parviporum*		EU189972	EU190082	EU190186	—	—	—
26719	American Type Culture Collection	*H. insulare*		DQ916076	DQ916091	DQ916105	EU190289	EU190290	1.8

[a] Collectors: NA, Naldo Anselmi; WB, William Bodles; JB, Johann Bruhn; GB, Guy Bussières; PC, Paolo Capretti; MG, Matteo Garbelotto; PG, Paolo Gonthier; NH, Nolan Hess; KK, Kari Korhonen; GL, Gaston Laflamme; PL, Piotr Łakomy; NL, Nicola Luisi; WO, William Otrosina; GS, Glen Stanosz; NHM, the National Herbarium of Mexico (El Herbario ENCB).

[b] Due to the low genetic diversity at this locus, only one representative sequence of each haplotype was submitted. Identical sequences noted by same accession number.

[c] ATP, mitochondrial ATP synthase subunit 6 gene; EFA, portion of the nuclear elongation factor 1-α gene; GPD, portion of the nuclear glyceraldehyde 3-phosphate dehydrogenase gene; MRI, portion of one of two non-homologous mitochondrial rDNA insertions in the ML5–ML6 region, two segments (seg1 and seg2) concatenated for analysis.

[d] Symbol "—", not sequenced or sequence unsuccessful.

[e] The insertion is present in two non-homologous forms of approximately 1.6 or 1.8 kb.

Table 2
PCR primers

Primer	Primer sequence (5′–3′)[a]	Reference	Region
ATP6-2	TAATTCTANWGCATCTTTAATRTA	Kretzer and Bruns (1999)	ATP synthase, subunit 6
ATP6-3	TCTCCTTTAGAACAATTTGA	Kretzer and Bruns (1999)	ATP synthase, subunit 6
Elongation factor 1-α F	TCAACGTGGTCGGTGAGCAGGTA	Johannesson and Stenlid (2003)	Elongation factor 1-α
Elongation factor 1-α R	AAGTCACGATGTCCAGGAGCATC	Johannesson and Stenlid (2003)	Elongation factor 1-α
GPD 1	AGCCTCTGCCCAYTTGAARG	This study	Glyceraldehyde 3-phosphate dehydrogenase
Glyceraldehyde 3-phosphate dehydrogenase R	RTANCCCCAYTCRTTRTCRTACCA	Johannesson et al. (2000)	Glyceraldehyde 3-phosphate dehydrogenase
Mito 7	GCCAATTTATTTTGCTACC	Gonthier et al. (2001)	Mitochondrial rDNA insertion
Mito f 212	ACTGTTACTAATCGAAAGTC	This study	Mitochondrial rDNA insertion

[a] Degeneracy codes: W = A or T, R = A or G, Y = C or T, N = A or T or C or G.

2.4. Phylogenetic analysis

Two separate types of phylogenetic reconstruction, maximum-parsimony (MP) and Bayesian methods, were utilized. If multiple isolates had identical sequences, only one was used in calculating single-gene genealogies. We assumed insertions and deletions (indels) to be single evolutionary events, therefore indels greater than two base-pairs in length were coded as a single character and weighted as equal to one base substitution. If sequences were biallelic due to heterozygous, heterokaryotic source material, and PCR products were not cloned prior to sequencing, sequences were coded using the degeneracy codes R = A or G, Y = C or T, etc. The closely related *H. insulare* was designated as the outgroup for all analyses except for the 1.6 kb rDNA insertion, which was not present in this isolate. In this case, *H. abietinum* was used as the outgroup.

For single-locus genealogies, MP trees were calculated using PAUP, version 4.0b10 (Swofford, 2000). MP trees were calculated using a heuristic search with tree bisection-reconnection (TBR) branch-swapping and 10 replicates with random sequence addition. For MP trees, internal branch support was assessed by bootstrap analysis of 1000 replicates with 10 random additions per replicate using the FastStep algorithm (Felsenstein, 1985).

To select the appropriate DNA sequence evolution model for each DNA region prior to Bayesian analysis, we utilized modeltest (Posada and Crandall, 1998). The Akaike information criterion (AIC) was used to assess model fit (Posada and Buckley, 2004). When the selected model was not implemented in MRBAYES, version 3.1 (Huelsenbeck and Ronquist, 2001), we employed the next-most complex model that was implementable. Models selected for GPD, EFA, ATP and both mitochondrial rDNA insertions were: GTR + I, HKY + I, F81 + I and GTR + I + Γ, respectively. All Bayesian tree reconstructions were performed using MRBAYES, version 3.1. Four Markov chain Monte Carlo chains—one cold and three heated, were run for 1,000,000 generations, sampling every 1000 generations. To assess where burn-in was reached, we plotted log likelihood scores versus generation number, and all samples prior to chain stationarity were excluded from subsequent tree-building. We performed two replicate runs. Fifty-percent majority-rule consensus trees were calculated, and branch support was assessed using Bayesian posterior probabilities.

For analysis of a combined dataset including DNA sequences from the three gene regions present in all isolates (GPD, EFA and ATP), including indel characters, we used the above Bayesian method. Partitioning data and allowing for parameter and rate heterogeneity within each partition can reduce systematic error introduced by application of an unpartitioned "compromise model" across divergent data (Brandley et al., 2005; Nylander et al., 2004). Therefore, data were divided into four partitions based first on data type—DNA versus standard, then by gene region within DNA. The model selected using modeltest under AIC, GTR + I + Γ, was specified such that estimated parameters and evolutionary rates could vary across all data partitions.

2.5. Network methods

Given the potential for reticulation among these closely related lineages, we also employed network reconstruction methods, which allow for incomplete reproductive isolation, recombination, multifurcation, or coexistence of ancestral and derived alleles (Posada and Crandall, 2001). We employed the median-joining network method for our study because of its robustness compared to other network methods in simulation studies using known gene genealogies (Cassens et al., 2003, 2005).

Median-joining network analyses were implemented in NETWORK, version 4.111 (Bandelt et al., 1999). This program includes an algorithm that infers missing, intermediate node haplotypes via maximum-parsimony criteria, thus circumventing lack of sampling of actual node haplotypes in the studied populations (Bandelt et al., 1999; Cassens et al., 2005). As the program does not accept multistate data, taxa with heterozygous sequence data were first removed from the datasets; the GPD dataset was not included in this analysis as a high proportion of the isolates were heterozygous in this DNA region. To prevent single indel events from being counted as multiple mutational steps, gap data were excluded from the calculations.

3. Results

With the exception of some Mexican herbarium specimens, target molecules were successfully sequenced for most isolates from which amplification was attempted. For North American isolates containing the insertion in the ML5–ML6 region of mitochondrial rDNA, 1930 to 1941 characters were analyzed depending on size of the insertion. Within this sequence dataset, 135 or 126 characters were parsimony informative, respectively. A total of 1185 characters, 91 of which were parsimony informative, were analyzed for Eurasian *H. annosum s.s.* isolates, lower counts than those for North America because all lack the mitochondrial rDNA insertion. Sequences were deposited in NCBI GenBank (Table 1).

3.1. Single-locus genealogies for ATP, EFA, GPD and mitochondrial rDNA insertions

There were 40,000 equally parsimonious GPD trees, 40,000 for EFA, three for ATP, 200 for the 1.6 kb mitochondrial rDNA insertion and 47 for the 1.8 kb insertion.

The North American *H. annosum* P ISG was phylogenetically distinct from Eurasian *H. annosum s.s.* in all single-gene genealogies computed by MP and Bayesian methods. The only exception to this pattern was the seven Castelporziano isolates; this group always clustered with North American *H. annosum* P ISG and never with the Eurasian clade. The analysis of the 1.6 kb DNA insertion, a region absent from all Eurasian *H. annosum s.s.* isolates, also placed Castelporziano isolates in the eastern North American clade. GPD phylogenetic analyses (Fig. 1) showed Eurasia and North America as sister groups as did EFA MP, however, EFA Bayesian analysis showed a North American clade within the Eurasian isolates (Fig. 2); MP analysis of ATP show separate continental clades, unresolved in a polytomy, while Bayesian analysis of this locus showed a Eurasian clade within a North American polytomy (Fig. 3).

Within North America, some individual analyses revealed evidence of intracontinental substructure. Neither MP nor Bayesian analyses of GPD data indicated phylogenetic structure within North America (Fig. 1). However, both phylogenetic analyses of EFA and ATP generally separate isolates with a provenance west of the Rocky Mountains from those originating east of the Rocky Mountains (Figs. 2 and 3). Exceptions were one eastern North American isolate and one western North American isolate that appeared in alternative clades in the EFA analysis, and two western North American isolates that appeared in the eastern North American clade in the ATP analysis. Analysis of the 1.6 kb rDNA insertion separated eastern from western North American isolates with a high degree of branch support using the two methods (Fig. 4A). Castelporziano isolates clustered with eastern North American isolates by sequence data from ATP, EFA and the 1.6 kb rDNA insertion. All non-Mexico western North American isolates for the 1.8 kb insertion have the same haplotype a haplotype absent from the sampled eastern isolates (Fig. 4B).

Analyses of Mexican samples unexpectedly revealed discrepancies of genotype placement based on different markers. All Mexican isolates clustered with ENA in the ATP analysis (Fig. 3). However, isolate ROL 503 had both eastern and western US alleles for the EFA region when cloned, and LOP 43 and REU 120 fell into their own strongly supported clade with the ENA (Fig. 2). NAV 464 was characterized by ENA alleles at all loci.

In contrast to the intracontinental patterns found in North America, Eurasian isolates did not show substructure related to geography in single-gene genealogies. Although there were distinct clades within the EFA and GPD genealogies, these clades were not partitioned based on the geographic sources of constituent isolates. Individuals from throughout the tested range in Eurasia: from the United Kingdom through Siberia, and from southern Italy through Scandinavia, intermingled in the Eurasian branches.

3.2. Bayesian phylogenetic analysis of the combined dataset

A Bayesian 50% majority-rule consensus tree of the combined dataset (Fig. 5) indicated all P-type isolates to be a monophyletic group with a posterior probability of 1.0. The constituent North American P and Eurasian P branches are each supported with a posterior probability of 1.0. Western North American P isolates formed a clade within the eastern isolates with a posterior probability of 1.0. The seven Castelporziano isolates formed a clade within the eastern North American P isolates, also supported with 100 percent probability. The only Mexican isolate with successful amplification of all three regions was located on a long branch within the eastern US isolates. While four non-Mexico isolates were placed in an incongruent clade based on single-locus analyses (above), only one had this pattern in the combined analysis—isolate 98008 from eastern Canada appeared in the western North American clade. Though several clades with varying degrees of support were present in the combined analysis, the Eurasian isolates showed no evidence of intracontinental structure related to geographic origin of the isolates.

3.3. Median-joining networks

We calculated median-joining (MJ) networks for the ATP, EFA and mitochondrial rDNA insertions with ambiguous sequences removed and gaps ignored. Each circular network node represents a single sequenced haplotype, with node size being proportional to number of isolates with that haplotype. Diamonds show unsampled nodes inferred by MJ network analysis, and tick marks on the branches show the number of mutations separating nodes. Network loops show either true reticulation events or alternative genealogies.

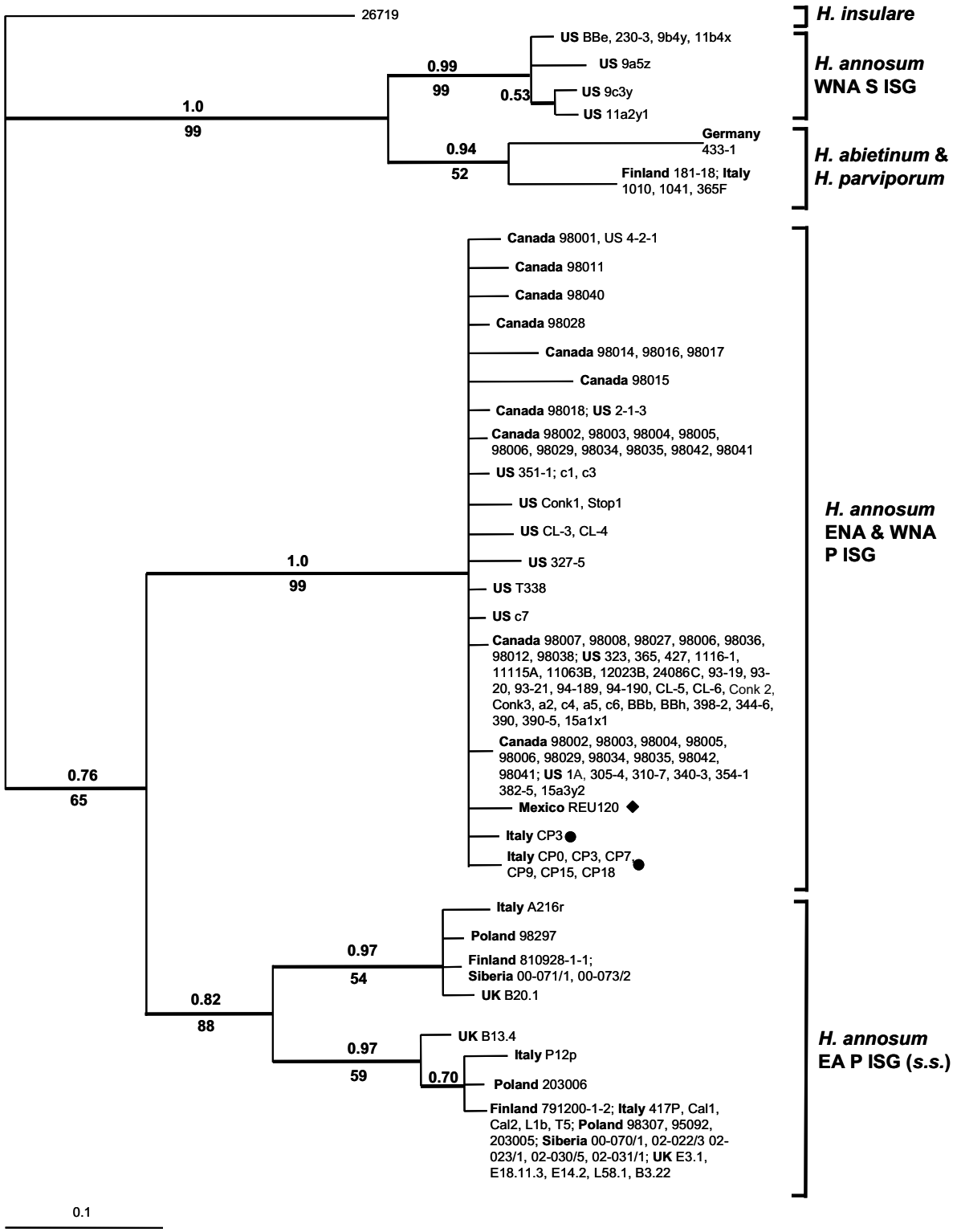

Fig. 1. Fifty-percent majority-rule Bayesian consensus phylogram for part of the nuclear glyceraldehyde 3-phosphate dehydrogenase gene. Thickest bold branches were supported in strict MP and 50% Bayesian consensus trees. Thinner bold branches were supported in only one type of consensus tree. Bootstrap values of 50 and above from 1000 replicates for MP analysis shown below the branches; posterior probabilities 0.5 or larger from 1,000,000 generation Bayesian analysis shown above the branches. Isolates from Castelporziano are marked with filled circles, the Mexican isolate with a filled diamond. WNA, western North America; ENA, eastern North America; EA, Eurasia. Outgroup is *H. insulare*.

The MJ network for the highly conserved mitochondrial ATP region consisted of eleven sampled haplotypes (Fig. 6A). Eurasian and western North American isolates branched off of an inferred node haplotype, and the four eastern North American haplotypes were one to two mutational steps removed from the western North American node.

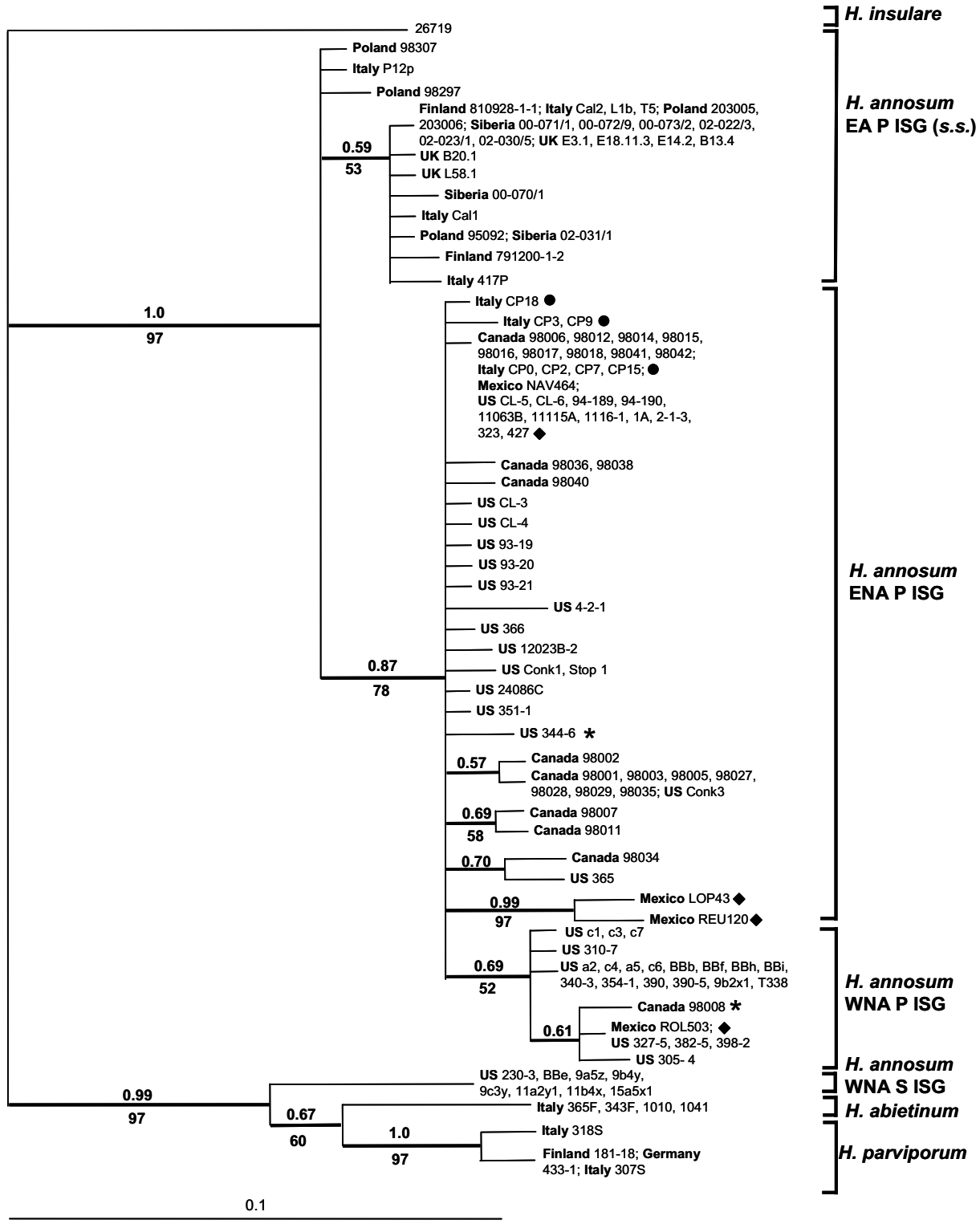

Fig. 2. Fifty-percent majority-rule Bayesian consensus phylogram for part of the nuclear elongation factor 1-α gene. Thickest bold branches were supported in strict MP and 50% Bayesian consensus trees. Thinner bold branches were supported in only one type of consensus tree. Bootstrap values of 50 and above from 1000 replicates for MP analysis shown below the branches; posterior probabilities 0.5 or larger from 1,000,000 generation Bayesian analysis shown above the branches. Isolates from Castelporziano are marked with filled circles, the Mexican isolates with filled diamonds. WNA, western North America; ENA, eastern North America; EA, Eurasia. Outgroup is *H. insulare*. *Isolates' clade incongruent with geographic origin—98008 = isolated ENA, 344-6 = isolated WNA.

All Castelporziano and Mexican isolates were part of an eastern North America node. The outgroup taxa were several mutational steps away from the P ISG portion of the network.

The EFA MJ network of 31 haplotypes (Fig. 6B) yielded all eastern North America haplotype nodes, including all of those from Castelporziano, in a coherent group intermedi-

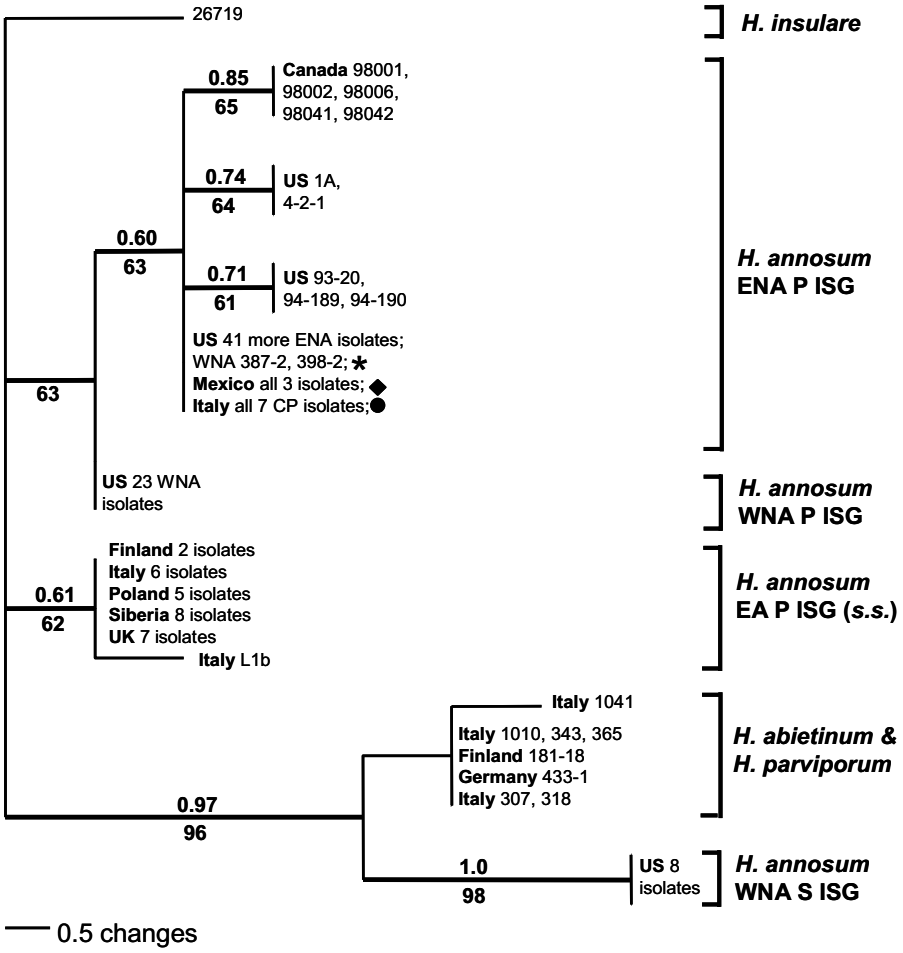

Fig. 3. Phylogram of one of three most parsimonious trees for part of the mitochondrial ATP synthase, subunit 6. Maximum-parsimony phylogram displayed here as NA P branch unsupported in Bayesian analysis. Thickest bold branches were supported in strict MP and 50% Bayesian consensus trees. Thinner bold branches were supported in only one type of consensus tree. Bootstrap values of 50 and above from 1000 replicates for MP analysis shown below the branches; posterior probabilities 0.5 or larger from 1,000,000 generation Bayesian analysis shown above the branches. Isolates from Castelporziano (CP) are marked with a filled circle, the Mexican isolates, with a filled diamond. WNA, western North America; ENA, eastern North America; EA, Eurasia. Outgroup is *H. insulare*. *Isolates' clade incongruent with geographic origin—387-2 and 398-2 = isolated WNA.

ate between those from western North America and Eurasia. The four haplotypes from Mexico were quite distinct with one included in an eastern North American node, one in a western North American node, and the remaining two haplotypes as separated nodes in the western cluster. Again, outgroup taxa in the EFA MJ network were separated from the *H. annosum* P ISG clusters by several mutations.

Thirty-four of the sequenced isolates contained the smaller mitochondrial rDNA insertion, yielding 18 distinct haplotypes (Fig. 6C). Again, this region is lacking in Eurasian *H. annosum s.s.*. In contrast to the GPD, EFA and ATP analysis, the P ISG haplotypes were removed from *H. annosum* S ISG by few mutational steps—in one case, only three. Western North American haplotypes were intermediate between this S ISG node and the eastern North American haplotypes. All Castelporziano sequences and one Mexican genotype were within the Eastern North American node. European *H. abietinum* and *H. parviporum* were several mutational steps away from the S ISG/P ISG section of the network. Fifty-one isolates contained the larger mitochondrial rDNA insertion, yielding 15 distinct haplotypes (Fig. 6D). The closest North American P ISG haplotype was five mutational steps removed from the S ISG node. The two Mexican isolates for which this region could be sequenced fell in distant parts of the network. All western North American isolates had a single haplotype located within the reticulate P ISG section.

4. Discussion

We document results of the most comprehensive study to date investigating the evolutionary history of pine-associated *H. annosum*, in terms of sample size, number and variety of analyzed loci and representation of worldwide range. In all single-gene genealogies, except the highly conserved mitochondrial ATP synthase coding region and one type of EFA tree, the pine-associated *H. annosum* represents a monophyletic group comprised of sister North American and Eurasian clades. MP phylogenetic analysis

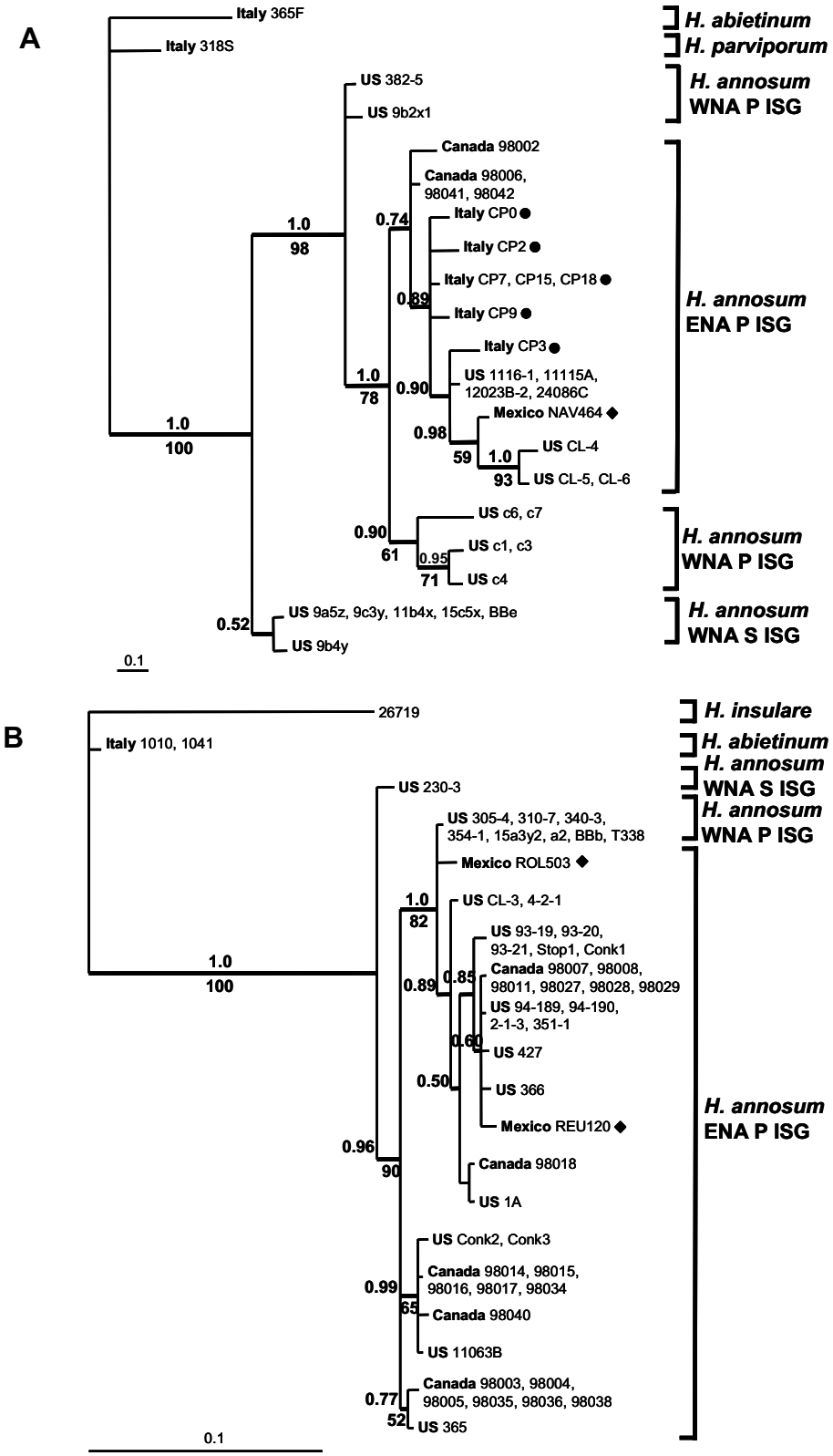

Fig. 4. Fifty-percent majority-rule phylogram of Bayesian analysis of 1.6 and 1.8 kb insertions into the mitochondrial ML5–ML6 region of rDNA. Partial, concatenated sequence. Thickest bold branches were supported in strict MP and 50% Bayesian consensus trees. Thinner bold branches were supported in only one type of consensus tree. Bootstrap values of 50 and above from 1000 replicates for MP analysis shown below the branches; posterior probabilities 0.5 or larger from 1,000,000 generation Bayesian analysis shown above the branches. Isolates from Castelporziano (CP) are marked with a filled circle, the Mexican isolates, with a filled diamond. WNA, western North America; ENA, eastern North America; EA, Eurasia. (A) 1.6 kb insertion. Outgroup is *H. abietinum*. (B) 1.8 kb insertion. Outgroup is *H. insulare.*

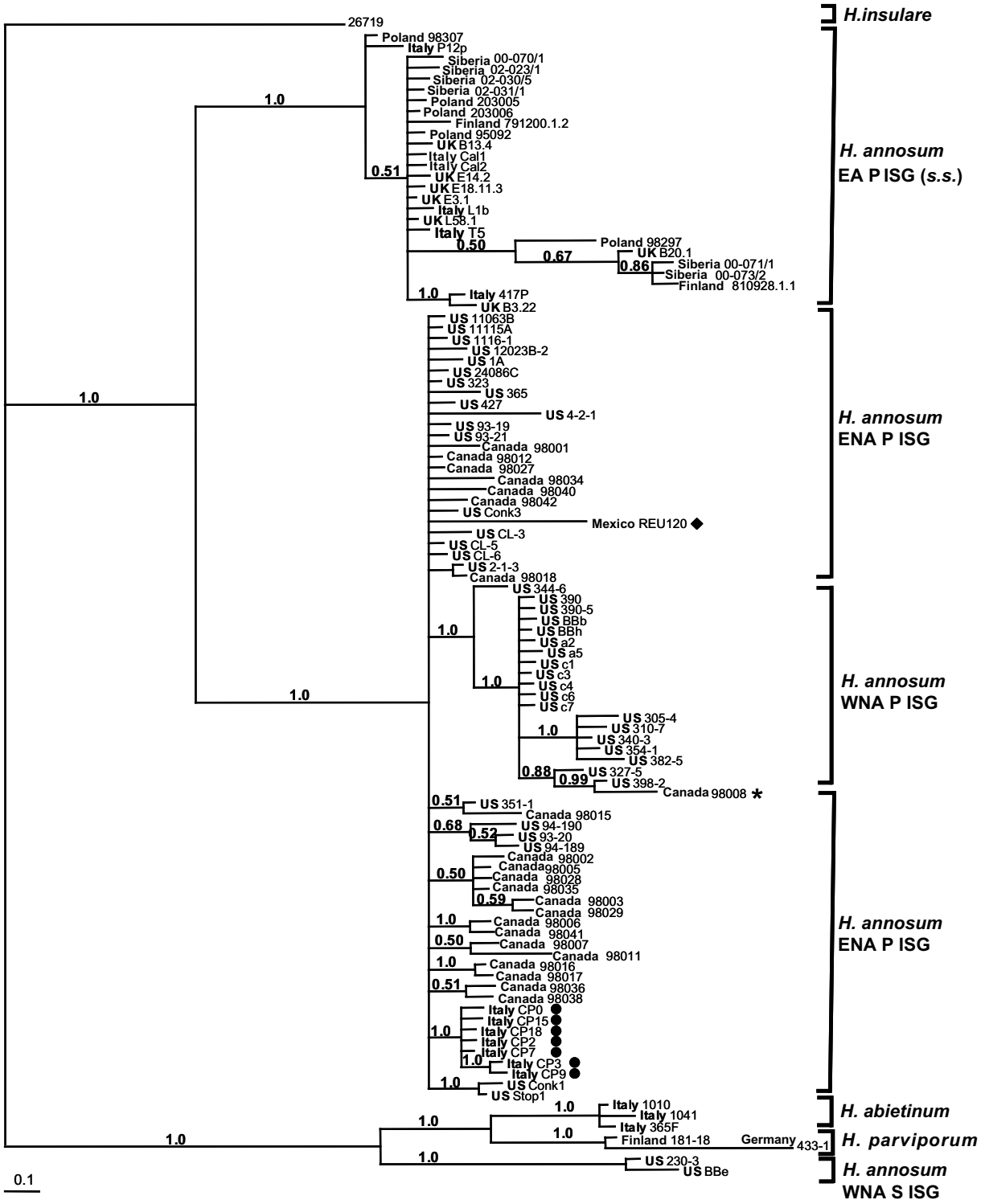

Fig. 5. Fifty-percent majority-rule phylogram of Bayesian analysis of partitioned, multilocus dataset: GPD, EFA and ATP. Calculations made with entire dataset; data divided into four partitions—standard, for indel data, and three different gene regions for the DNA sequence data. Posterior probabilities larger than 0.5 from 1,000,000 generations of Bayesian analysis are shown above the branches. Isolates from Castelporziano are marked with filled circles, the Mexican isolate with a filled diamond. WNA, western North America; ENA, eastern North America; EA, Eurasia. Outgroup is *H. insulare*. *Clade placement of ENA isolate 98008 incongruent with geographic origin.

of the ATP synthase sequence data differentiates the two continental clades, but places them in a polytomy with other taxa within the complex. The North American branch is not supported in the Bayesian consensus tree. The limited resolution of the ATP analysis is likely due to the limited polymorphism levels present. In the analysis of the combined data, including the ATP sequences, the P ISG is monophyletic with 100% posterior probability and

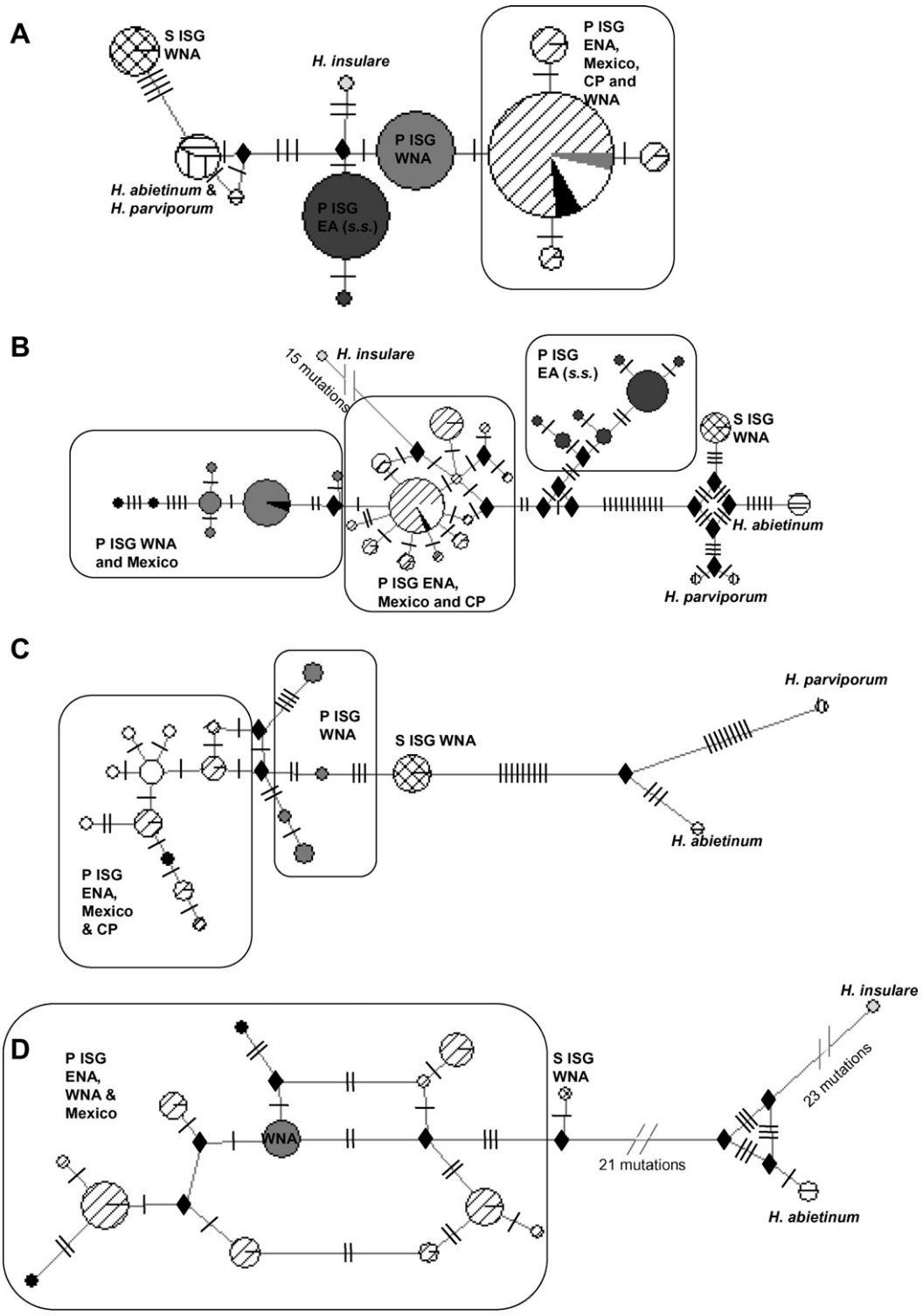

Fig. 6. Median-joining networks. Each circular node represents a distinct haplotype, and node size is proportional to number of individuals of that haplotype. Tick marks along branches indicate number of mutational changes between nodes; filled diamond nodes are unsampled haplotypes inferred during analysis. S ISG WNA (cross-hatched), *H. annosum* S ISG; light gray, *H. insulare*; horizontal stripes, *H. abietinum*; vertical stripes, *H. parviporum*; P ISG EA (*s.s.*) (dark gray), Eurasian *H. annosum s.s.*; P ISG WNA (medium gray), western North American *H. annosum* P ISG; P ISG ENA (diagonal stripes), eastern North American *H. annosum* P ISG; CP (white), Italian Castelporziano isolates; black, Mexican isolates. (A) Mitochondrial ATP synthase subunit 6 coding region network. The largest eastern North American *H. annosum* P ISG node contains three Mexican isolates, seven Castelporziano isolates and two western North American isolates. (B) Nuclear elongation factor 1-α network. (C) Mitochondrial rDNA 1.6 kb insertion network. (D) Mitochondrial rDNA 1.8 kb insertion network.

has well-supported sister Eurasian and North American groups. Our results confirm the genetic differentiation between North American and Eurasian P shown by isozyme studies and phylogenetic analysis of ITS/IGS and some manganese peroxidase paralogs (Harrington et al., 1998; Karlsson and Stenlid, 1991; Maijala et al., 2003; Otrosina et al., 1993). Phylogenetic studies of putative pathogenicity-related laccase genes did not show separation between North American and Eurasian P ISG (Asiegbu et al., 2004), but the lack of separation may be due to differential selection pressures on this wood-degradation enzyme.

These results offer insight regarding unresolved problems in *H. annosum s.l.* taxonomy. Increasingly, designation of divergent fungal taxa is being performed using several methods of species recognition concurrently, including phylogenic patterns, reproductive isolation and phenotypic characters (Dettman et al., 2003a,b; Harrington and Rizzo, 1999; Taylor et al., 2000). Various combinations of host preference, intersterility and population differentiation have been used to designate separations in the *H. annosum s.l.* complex. Currently, there are five major *H. annosum s.l.* lineages, two of which have been given separate species names.

Whether the two P ISG lineages, *H. annosum s.s.* and the North American P ISG, should be considered distinct species has been an open question. The evidence supporting a common nomenclature for both groups includes their monophyly, nearly complete interfertility, phenotypic similarities, close levels of genetic relatedness, and similar host range and mode of pathogenicity. However, the Eurasian and North American populations are differentiated into two clear sister taxa with no evidence of recent gene flow. Aside from Castelporziano individuals, no tested isolates of North American origin ever clustered in the Eurasian clade. Moreover, the severe disease caused by exotic North American genotypes in Italy (Gonthier et al., 2004, 2007) suggests that the two taxa have significantly diverged in allopatry, each lineage acquiring unique phenotypic traits. If *H. annosum s.s.* is to continue to be used for both North American and Eurasian taxa, we propose assigning subspecies qualifiers to acknowledge these differences. Given that genetic isolation often precedes morphological distinctions and reproductive isolation in microbes (Taylor et al., 2006), separate species names may be most appropriate for these two distinct phylogenetic species. This distinction may assist regulators in preventing further intercontinental introductions.

In contrast to the monophyletic nature of European *H. annosum s.s.* and North American *H. annosum* P ISG, evolutionary relationships among the European *H. abietinum*, *H. parviporum* and the North American *H. annosum* S ISG are not completely resolved. Using broad geographic sampling of the three taxa, a multilocus combined phylogenetic analysis of nuclear loci showed support for sister *H. parviporum* and North American *H. annosum* S ISG clades as the sister clade to *H. abietinum* (Johannesson and Stenlid, 2003). Evidence of alternate relationships is found in our own dataset, including mitochondrial sequences, some single nuclear loci (Johannesson and Stenlid, 2003; Ota et al., 2006) and the ITS and IGS regions (Harrington et al., 1998). In our and all cited studies, however, the lineages currently designated *H. annosum s.l.* are paraphyletic, justifying the need for a different specific designation for the North American *H. annosum* S ISG.

At an intracontinental geographic scale, we found evidence of a subdivision in North America between P ISG isolates originating from east vs. west of the Rocky Mountains. Although weak branch support or clade instability under different phylogenetic reconstruction methods makes this relationship somewhat ambiguous in individual gene genealogies, the separation of the western from the eastern clade was strongly supported in analysis of the combined dataset. The two populations may be evolving towards more complete separation. While a few North American isolates fell into incongruent clades in analyses of individual loci, only one eastern Canadian isolate was placed in the western North American clade in the multilocus analysis. The reason for this placement is unclear. We cannot differentiate between the presence of rare ancestral alleles and more recent, long-distance movement of fungal isolates between the two regions. The possibility that *H. annosum* may have been successfully transported across the continent warrants the need to elucidate potential routes of movement.

Our data provide some evidence to address the origin and dispersal history of the P ISG lineage. At least six *Heterobasidion* taxa are indigenous in Eurasia as opposed to two in North America, which has been used to propose a Eurasian origin for the *Heterobasidion* genus (Korhonen and Dai, 2005). Although EFA Bayesian analysis suggests the North American taxon arose from within the Eurasian, the two are sister groups in other phylogenetic analysis, including the combined analysis. Hence we limit ourselves to the inference that the common ancestor of the two P ISG sister clades may have arisen in Eurasia, diversifying from the F and S ISG lineages there. The ancestral P ISG population may have then separated, with the current *H. annosum s.s.* lineage colonizing western Eurasia and another lineage dispersing over a land bridge to found the North American P ISG populations. Dispersal likely occurred over a Beringean land bridge, as the last terrestrial connection between North America and Europe was severed during the Eocene, approximately 50 MYA (Knox, 1998). Such ancient isolation would likely have resulted in much higher genetic divergence between the two groups. Phylogenetic analysis of the ITS region provides some evidence that an Australian taxon, *H. araucariae*, is basal to the *H. insulare*/*H. annosum s.l.* species complexes (Harrington et al., 1998), making it unlikely that North America is the geographic source of the Eurasian *H. annosum s.s.* lineages. The relative position of *H. araucariae*, however, is different in a multilocus analysis using nuclear genes (Ota et al., 2006). Adding more basal relatives into a rigorous,

multilocus phylogenetic study is necessary to allow us to distinguish between hypothesized orders and directions of events in the history of all *Heterobasidion* lineages.

In North America, Mexico contains both ENA and WNA alleles and has higher genetic divergence among the four analyzed isolates than was sampled in either the eastern or western North American populations. Thus, our data suggest Mexican isolates represent an evolutionary bridge between the two. Moreover, the western North American clade is nested within the eastern North American P ISG clade. Two alternative scenarios could then account for the spread of this organism within North America. Arriving from Eurasia, the P ISG may have first dispersed southward in eastern North America through Mexico and then northward to western North America. Alternatively, a widespread North American P may have been confined to Mexico during a period of glaciation, later recolonizing both eastern and western North America, resulting in the two divergent lineages. The high genetic diversity and variable clade placement observed among the few Mexican isolates we were able to include in this study seems to support the latter scenario. However, the nesting of the western North American clade within the eastern clade in the combined Bayesian analysis supports the first scenario. Interestingly, the mitochondrial ATP analyses point to the eastern North American isolates potentially being derived from the western isolates, hence the mitochondria may have a different history than the sequenced nuclear loci. A landscape-scale, empirical study of potential North American glacial refugia and recolonization pathways points to Mexico as harboring such a refuge during past glaciation (Swenson and Howard, 2005). Studies utilizing additional Mexican isolates, more variable DNA regions or markers suited to population-level analyses are needed to determine the most probable hypothesis.

The patterns of inter- and intracontinental biogeographical structure between Eurasia and North America identified here for the *H. annosum* P ISG agree with those observed in numerous additional fungi. For example, a multilocus phylogenetic study of *Amanita muscaria* and *A. pantherina*, both of which can establish an ectomycorrhizal (EM) relationship with members of *Pinaceae*, displayed a pattern very similar to that of the worldwide P ISG. Intracontinental relationships within Eurasia and North America were closer than intercontinental ones, though another study of *A. muscaria* revealed an Alaskan region of lineage coexistence (Geml et al., 2006; Oda et al., 2004). Moreover, the *A. muscaria* clade within North America also has a subclade of western North American isolates within the eastern North American group, with eastern North America falling between western North America and Eurasia, suggesting continental connectivity via a Beringean or North Atlantic land bridge (Oda et al., 2004). As P ISG populations are only found as far north as the US state of Washington in North America, the *H. annosum* pattern is also reminiscent of the one reported for the matsutake mushroom species complex (genus *Tricholoma*), which can also form an EM relationship with some conifers (Chapela and Garbelotto, 2004). Eurasian matsutake populations are more closely related to eastern North American individuals than to those from western North America, and Mexican isolates are intermediate between a circumboreal group, including eastern US individuals, and a western US clade. In contrast to the P ISG, however, the group likely evolved in western North America dispersing westward over a Bering Straight land bridge (Chapela and Garbelotto, 2004). Phylogenetic reconstructions for two other lignicolous basidiomycetes, *Artomyces pyxidatus* and *Armillaria mellea*, show distinct Eurasian and North American clades. The North American clades are divided between eastern and western clusters, although possible dispersal or vicariance pathways among the clades are obscure (Coetzee et al., 2000; Lickey et al., 2002). Thus, many basidiomycetes, including several associated with conifers, demonstrate closer intracontinental than intercontinental phylogeographical relationships. Moreover, at the intracontinental scale, the frequency of phylogenetic divisions between eastern and western isolates within many North American clades suggests that the Rocky Mountains and the Great Plains constitute a barrier to gene flow for many fungal taxa.

Our phylogenetic analyses also revealed evidence of two events that likely occurred after the ancient divergence of the major *Heterobasidion* lineages. The first is a possible instance of horizontal genetic transfer, and the second is a recent intercontinental introduction and establishment of the North American P ISG in Italy. The highly variable mitochondrial rDNA insertions display a very different pattern than the other mitochondrial and nuclear gene regions. Both forms of the non-exonic insertion, though located in the same part of the gene, are completely non-homologous, and both are absent from all Eurasian *H. annosum s.s.* isolates. The smaller rDNA insertion is closely related to that found in the *H. annosum* S ISG: in the MJ network, a western North American P ISG isolate is intermediate between the rest of the P ISG and the western North American S SIG isolates (Fig. 6C). Though the MJ network for the larger insertion is markedly reticulated, the S ISG genotype is only five mutational steps away from the nearest North American P ISG genotype, while *H. insulare* is 51 steps from any North American P (Fig. 6D). By contrast, analyses of all other loci show the North American P ISG isolates separated from the S ISG isolates by many mutational changes, and the S ISG genotypes are closest to *H. abietinum* and *H. parviporum*. This pattern is apparent in the highly conserved mitochondrial ATP region (Figs. 3 and 6A) and in the nuclear loci (Figs. 1, 2 and 6B). The fact that S ISG rDNA insertion sequences are closest to North American P ISG sequences suggests an instance of horizontal transfer of the insertions. As the west is the only North American region in which both ISGs are in sympatry, the P ISG lineage may have acquired these insertions from the S ISG lineage after introduction from Eurasia. Potential mechanisms for the transfer of an

independent segment of S SIG-type mitochondrial DNA include mitochondrial recombination or the movement of mobile DNA elements. Both of these scenarios have been identified in fungal mitochondria, particularly for taxa in which hybridization can lead to heteroplasmy (reviewed in Barr et al., 2005). Notably, the only stable, inter-ISG hybrid found in nature to date is an SP hybrid isolated in the western US, demonstrating the possibility that these ISGs can cross outside of the laboratory. Alternately, this DNA segment may have been lost from the Eurasian P ISG lineage. This, however, does not explain the closeness of the North American P to the North American S and the distance of the S from *H. abietinum* and *H. parviporum*, a pattern at odds with other sequenced loci from this study and analysis of molecular markers from numerous other *Heterobasidion* studies.

We have previously identified seven genotypes from Castelporziano (Italy) as ENA, based on a phylogenetic analysis that employed a more limited set of samples (Gonthier et al., 2004; Warner et al., 2005). The ENA origin of these isolates is fully supported by the broader phylogenetic and MJ network analyses reported here. As all of the Castelporziano Estate isolates form a separate clade within the eastern North American isolates in the combined tree, these isolates may either originate from an area not sampled in this study or may have diverged slightly since their introduction to the site. Rapid evolution often occurs as introduced populations respond to novel abiotic and biotic conditions (Sakai et al., 2001), and may explain the differentiation. It is also possible that gene flow may have occurred between the introduced ENA genotypes and the native Italian genotypes since the hypothesized introduction, and indeed, evidence of hybridization has been found recently (Gonthier et al., 2007). The estate has been closed to the public for centuries and contains only native plants, precluding an introduction linked to exotic plantings. As previously suggested, the most likely mode of introduction is via untreated wood associated with the US Army regiment encampment on the grounds in 1944, during World War II (Gonthier et al., 2004). The ability to assign an exotic pathogen to a region of origin may assist us in better understanding its biology and preventing further introductions (Wingfield et al., 2001).

Acknowledgements

We gratefully acknowledge the funding source for this work, a PSW (FS Region 5) Technological Improvement grant. We thank Naldo Anselmi, William Bodles, Paolo Capretti, Kari Korhonen, Piotr Łakomy, Nicola Luisi, Jeanne Mihail, Dionicio Alvarado Rosales, Glen Stanosz, Stephen Woodward and the National Herbarium of Mexico (El Herbario ENCB) for generously helping us to obtain study material. Thanks also to Fabio Guglielmo and Carlos Rodarte for technical assistance. We thank two anonymous reviewers for helpful comments on the manuscript.

References

Asiegbu, F.A., Abu, S., Stenlid, J., Johansson, M., 2004. Sequence polymorphism and molecular characterization of laccase genes of the conifer pathogen *Heterobasidion annosum*. Mycol. Res. 108, 136–148.

Avise, J., 2000. Phylogeography: The History and Formation of Species. Harvard University Press, Cambridge, Massachusetts.

Bandelt, H.J., Forster, P., Röhl, A., 1999. Median-joining networks for inferring intraspecific phylogenies. Mol. Biol. Evol. 16, 37–48.

Barr, C.M., Neiman, M., Taylor, D.R., 2005. Inheritance and recombination of mitochondrial genomes in plants, fungi and animals. New Phytol. 168, 39–50.

Brandley, M.C., Schmitz, A., Reeder, T., 2005. Partitioned Bayesian analyses, partition choice and phylogenetic relationships of scincid lizards. Syst. Biol. 54, 373–390.

Capretti, P., Korhonen, K., Mugnai, L., Romagnoli, C., 1990. An intersterility group of *H. annosum* specialized to *Abies alba*. Eur. J. Forest Pathol. 20, 231–240.

Cassens, I., Mardulyn, P., Milinkovitch, M.C., 2005. Evaluating intraspecific "network" construction methods using simulated sequence data: do existing algorithms outperform the global maximum parsimony approach? Syst. Biol. 54, 363–372.

Cassens, I., Van Waerebeek, K., Best, P.B., Crespo, E.A., Reyes, J., Milinkovitch, M.C., 2003. The phylogeography of dusky dolphins (*Lagenorhynchus obscurus*): a critical examination of network methods and rooting procedures. Mol. Ecol. 12, 1781–1792.

Chapela, I.H., Garbelotto, M., 2004. Phylogeography and evolution in matsutake and close allies inferred by analysis of ITS sequences and AFLPs. Mycologia 96, 730–741.

Chase, T.E., Ullrich, R.C., 1990. Five genes determining intersterility in *Heterobasidion annosum*. Mycologia 82, 73–91.

Coetzee, M.P.A., Wingfield, B.D., Harrington, T.C., Dalevi, D., Coutinho, T.A., Wingfield, M.J., 2000. Geographical diversity of *Armillaria mellea* s.s. based on phylogenetic analysis. Mycologia 92, 105–113.

Coetzee, M.P.A., Wingfield, B.D., Harrington, T.C., Steimel, J., Coutinho, T.A., Wingfield, M.J., 2001. The root rot fungus, *Armillaria mellea*, introduced into South Africa by early Dutch settlers. Mol. Ecol. 10, 387–396.

Crouch, J.A., Clarke, B.B., Hillman, B.I., 2006. Unraveling the evolutionary relationships among the divergent lineages of *Colletotrichum* causing anthracnose disease in turfgrass and corn. Phytopathology 96, 46–60.

Dettman, J.R., Jacobson, D.J., Taylor, J.W., 2003a. A multilocus genealogical approach to phylogenetic species recognition in the model eukaryote *Neurospora*. Evolution 57, 2703–2720.

Dettman, J.R., Jacobson, D.J., Turner, E., Pringle, A., Taylor, J.W., 2003b. Reproductive isolation and phylogenetic divergence in *Neurospora*: comparing methods of species recognition in a model eukaryote. Evolution 57, 2721–2741.

Felsenstein, J., 1985. Confidence intervals on phylogenies: an approach using the bootstrap. Evolution 39, 783–791.

Fisher, M.C., Koenig, G.L., White, T.J., San-Blas, G., Negroni, R., Alvarez, I.G., Wanke, B., Taylor, J.W., 2001. Biogeographic range expansion into South America by *Coccidiodes immitis* mirrors New World patterns of human migration. Proc. Natl. Acad. Sci. USA 98, 4558–4562.

Garbelotto, M., 2004. Root and butt rot diseases. In: Burley, J., Evans, J., Youngquist, J.A. (Eds.), The Encyclopedia of Forest Sciences, vol. 2. Elsevier, Oxford, pp. 750–758.

Garbelotto, M., Ratcliff, A., Bruns, T.D., Cobb, F.W., Otrosina, W.J., 1996. Use of taxon-specific competitive-priming PCR to study host specificity, hybridization, and intergroup gene flow in intersterility groups of *Heterobasidion annosum*. Phytopathology 86, 543–551.

Garbelotto, M., Gonthier, P., Linzer, R., Nicolotti, G., Otrosina, W., 2004. A shift in nuclear state as the result of natural interspecific hybridization between two North American taxa of the basidiomycete complex *Heterobasidion*. Fungal Genet. Biol. 41, 1046–1051.

Geml, J., Laursen, G.A., O'Neill, K., Nusbaum, H.C., Taylor, D.L., 2006. Beringian origins and cryptic speciation events in the fly agaric (*Amanita muscaria*). Mol. Ecol. 15, 225–239.

Gonthier, P., Garbelotto, M., Varese, G.C., Nicolotti, G., 2001. Relative abundance and potential dispersal range of *Heterobasidion annosum* in pure and mixed forests. Can. J. Bot. 79, 1057–1065.

Gonthier, P., Warner, R., Nicolotti, G., Mazzaglia, A., Garbelotto, M., 2004. Pathogen introduction as a collateral effect of military activity. Mycol. Res., 468–470.

Gonthier, P., Nicolotti, G., Linzer, R., Guglielmo, F., Garbelotto, M., 2007. Invasion of European pine stands by a North American forest pathogen and its hybridization with a native interfertile taxon. Mol. Ecol. 16, 1389–1400.

Harrington, T.C., Rizzo, D.M., 1999. Defining species in the fungi. In: Worrall, J. (Ed.), Structure and Dynamics of Fungal Populations. Kluwer Academic Publishers, Dordrecht, pp. 43–71.

Harrington, T.C., Stenlid, J., Korhonen, K., 1998. Evolution in the genus *Heterobasidion*. In: Delatour, C., Guillaumin, J.J., Lung-Escarmant, B., Marcais, B. (Eds.), Root and Butt Rots of Forest Trees: Proceedings of the 9th International Conference on Root and Butt Rot. INRA, France, pp. 63–74.

Hayden, K.J., Rizzo, D., Tse, J., Garbelotto, M., 2004. Detection and quantification of *Phytophthora ramorum* from California forests using a real-time polymerase chain reaction assay. Phytopathology 94, 1075–1083.

Huelsenbeck, J.P., Ronquist, F., 2001. MRBAYES: Bayesian inference of phylogenetic trees. Bioinformatics 17, 754–755.

Johannesson, H.S., Johannesson, K.H.P., Stenlid, J., 2000. Development of primer sets to amplify fragments of conserved genes for use in population studies of the fungus *Daldinia loculata*. Mol. Ecol. 9, 375–377.

Johannesson, H.S., Stenlid, J., 2003. Molecular markers reveal genetic isolation and phylogeography of the S and F intersterility groups of the wood decay fungus *Heterobasidion annosum*. Mol. Phylogenet. Evol. 29, 94–101.

Karlsson, J.-O., Stenlid, J., 1991. Pectic enzyme profiles of intersterility groups in *Heterobasidion annosum*. Mycol. Res. 95, 531–536.

Kasuga, T., White, T.J., Koenig, G., McEwen, J., Restrepo, A., Castañeda, E., Da Silva Lacaz, C., Heins-Vaccari, E.M., De Freitas, R.S., Zancopé-Oliveira, R.M., Qin, Z., Negroni, R., Carter, D.A., Mikami, Y., Tamura, M., Taylor, M.L., Miller, G.F., Poonwan, N., Taylor, J.W., 2003. Phylogeography of the fungal pathogen *Histoplasma capulatum*. Mol. Ecol. 12, 3383–3401.

Kauserud, H., Högberg, N., Knudsen, H., Elborne, S.A., Schumacher, T., 2004. Molecular phylogenetics suggest a North American link between the anthropogenic dry rot fungus *Serpula lacrymans* and its wild relative *S. himantioides*. Mol. Ecol. 13, 3137–3146.

Knox, R.W.O'B., 1998. The tectonic and volcanic history of the North Atlantic region during the Paleocene—Eocene transition: implications for NW European and global biotic events. In: Aubry, M.P., Lucan, S.G., Berggren, W.A. (Eds.), Late Paleocene—Early Eocene Climatic and Biotic Events in the Marine and Terrestrial Records. Columbia University Press, New York, pp. 91–102.

Kohn, L.M., 2005. Mechanisms of fungal speciation. Annu. Rev. Phytopathol. 43, 279–308.

Korhonen, K., 1978. Intersterility groups of *Heterobasidion annosum*, vol. 94. Communicationes Instituti Forestalis Fenniae, 25 pp.

Korhonen, K., Bobko, I., Hanso, I., Piri, T., Vasiliauskas, A., 1992. Intersterility groups of *Heterobasidion annosum* in some spruce and pine stands in Byelorussia, Lithuania and Estonia. Eur. J. Forest Pathol. 22, 384–391.

Korhonen, K., Stenlid, J., 1998. Biology of *Heterobasidion annosum*. In: Woodward, S., Stenlid, J., Karjalainen, R., Hütterman, A. (Eds.), *Heterobasidion annosum*: Biology, Ecology, Impact and Control. CAB International, Wallingford, pp. 43–70.

Korhonen, K., Dai, Y.-C., 2005. Genetically identified taxa of *Heterobasidion* and their distribution in Eurasia. In: Mańka, M., Łakomy, P. (Eds.), Root and Butt Rots of Forest Trees. Proceedings of the 11th International Conference on Root and Butt Rots. The August Cieszkowski Agricultural University, Poznań, pp. 57–63.

Kretzer, A.M., Bruns, T.D., 1999. Use of *atp*6 in fungal phylogenetics: and example from the Boletales. Mol. Phylogenet. Evol. 13, 483–492.

Lickey, E.B., Hughes, K.W., Petersen, R.H., 2002. Biogeographical patterns in *Artomyces pyxidatus*. Mycologia 94, 461–471.

Maijala, P., Harrington, T.C., Raudaskoski, M., 2003. A peroxidase gene family and gene trees in *Heterobasidion* and related genera. Mycologia 95, 209–221.

Methven, A., Hughes, K.W., Petersen, R.H., 2000. *Flammulina* RFLP patterns identify species and show biogeographical patterns within species. Mycologia 92, 1064–1070.

Niemelä, T., Korhonen, K., 1998. Taxonomy of the Genus *Heterobasidion*. In: Woodward, S., Stenlid, J., Karjalainen, R., Hütterman, A. (Eds.), *Heterobasidion annosum*: Biology, Ecology, Impact and Control. CAB International, Wallingford, pp. 27–33.

Nylander, J.A.A., Ronquist, F., Huelsenbeck, J.P., Nieves-Aldrey, J.L., 2004. Bayesian phylogenetic analysis of combined data. Syst. Biol. 53, 47–67.

Oda, T., Tanaka, C., Tsuda, M., 2004. Molecular phylogeny and biogeography of the widely distributed *Amanita* species, *A. muscaria* and *A. pantherina*. Mycol. Res. 108, 885–896.

Ota, Y., Tokuda, S., Buchanan, P.K., Hattori, T., 2006. Phylogenetic relationships of Japanese species of *Heterobasidion–H. annosum sensu lato* and an undetermined *Heterobasidion* sp. Mycologia 98, 717–725.

Otrosina, W.J., Chase, T.E., Cobb Jr., F.W., Korhonen, K., 1993. Population structure of *Heterobasidion annosum* from North America and Europe. Can. J. Bot. 71, 1064–1071.

Petersen, R.H., Hughes, K.W., 2003. Phylogeographic examples of Asian biodiversity in mushrooms and their relatives. Fungal Divers. 13, 95–109.

Posada, D., Crandall, K.A., 1998. Modeltest: testing the model of DNA substitution. Bioinformatics 14, 817–818.

Posada, D., Crandall, K.A., 2001. Intraspecific gene genealogies: trees grafting into networks. Trends Ecol. Evol. 16, 37–45.

Posada, D., Buckley, T.R., 2004. Model selection and model averaging in phylogenetics: advantages of Akaike information criterion and Bayesian approaches over Likelihood Ratio Tests. Syst. Biol. 53, 793–808.

Pratt, J.E., Greig, B.J.W., 1988. *Heterobasidion annosum*: development of butt rot following thinning in two young first rotation stands of Norway spruce. Forestry 61, 339–347.

Rambaut, A., 1996. Se–Al: Sequence Alignment Editor. Available http://evolve.zoo.ox.ac.uk/.

Sakai, A.K., Allendorf, F.W., Holt, J.S., Lodge, D.M., Molofsky, J., With, K.A., Baughman, S., Cabin, R.J., Cohen, J.E., Ellstrand, N.C., McCauley, D.E., O'Neil, P., Parker, I.M., Thompson, J.N., Weller, S.G., 2001. The population biology of invasive species. Annu. Rev. Ecol. Syst. 32, 305–332.

Stenlid, J., Karlsson, J.-O., 1991. Partial intersterility in *Heterobasidion annosum*. Mycol. Res. 95, 1153–1159.

Stenlid, J., Redfern, D.B., 1998. Spread within the tree and stand. In: Woodward, S., Stenlid, J., Karjalainen, R., Hütterman, A. (Eds.), *Heterobasidion annosum*: Biology, Ecology, Impact and Control. CAB International, Wallingford, pp. 125–141.

Stenlid, J., Swedjemark, G., 1988. Differential growth of S- and P-isolates of *Heterobasidion annosum* in *Picea abies* and *Pinus sylvestris*. Trans. Br. Mycol. Soc. 90, 209–213.

Swenson, N.G., Howard, D.J., 2005. Clustering of contact zones, hybrid zones and phylogeographic breaks in North America. Am. Nat. 166, 581–591.

Swofford, D.L., 2000. PAUP*: phylogenetic analysis using parsimony (* and other methods). Version 4.0b10. Sinauer Associates, Sunderland, Massachsetts.

Taylor, J.W., Jacobson, D.J., Kroken, S., Kasuga, T., Geiser, D.M., Hibbett, D.S., Fisher, M.C., 2000. Phylogenetic species recognition and concepts in fungi. Fungal Genet. Biol. 31, 21–32.

Taylor, J.W., Turner, E., Townsend, J.P., Dettman, J.R., Jacobson, D., 2006. Eukaryotic microbes, species recognition and the geographic

limits of species: examples from the kingdom Fungi. Philos. Trans. R. Soc. B 361, 1947–1963.

Vilgalys, R., Sun, B.L., 1994. Ancient and recent patterns of geographic speciation in the oyster mushroom *Pleurotus* revealed by phylogenetic analysis of ribosomal DNA sequences. Proc. Natl. Acad. Sci. USA 91, 4599–4603.

Warner, R., Gonthier, P., Otrosina, W., Laflamme, G., Bussières, G., Bruhn, J., Garbelotto, M., 2005. Phylogenetic analysis of *Heterobasidion annosum* P ISG from an inter- to an intracontinental scale. In: Mańka, M., Łakomy, P. (Eds.), Root and Butt Rots of Forest Trees. Proceedings of the 11th International Conference on Root and Butt Rots. The August Cieszkowski Agricultural University, Poznań, pp. 64–72.

Wingfield, M.J., Slippers, B., Roux, J., Wingfield, B.D., 2001. Worldwide movement of exotic forest fungi, especially in the tropics and the Southern Hemisphere. BioScience 51, 134–140.

Wu, Q.-X., Mueller, G.M., Lutzoni, F.M., Huang, Y.-Q., Guo, S.-Y., 2000. Phylogenetic and biogeographic relationships of eastern Asian and eastern North American disjunct *Suillus* species (Fungi) as inferred from nuclear ribosomal RNA ITS sequences. Mol. Phylogenet. Evol. 17, 37–47.

Zervakis, G.I., Moncalvo, J., Vilgalys, R., 2004. Molecular phylogeny, biogeography and speciation of the mushroom species *Pleurotus cystidiosus* and allied taxa. Microbiology 150, 715–726.